https://doi.org/10.1016/j.ijthermalsci.2016.11.008

Heat conduction with fractional Cattaneo–Christov upper-convective derivative flux model

Lin Liu [a, b], Liancun Zheng [b *], Fawang Liu [c], Xinxin Zhang [a]

[a] School of Mechanical Engineering, University of Science and Technology Beijing, Beijing 100083, China

[b] School of Mathematics and Physics, University of Science and Technology Beijing, Beijing 100083, China

[c] School of Mathematical Sciences, Queensland University of Technology, GPO Box 2434, Brisbane, Qld. 4001, Australia

Abstract: Fractional order derivative operators are global ones that the time fractional one possesses memory character while the space one reflects non-local character. In this paper, a new fractional constitutive model is suggested in the investigation of heat conduction with Cattaneo–Christov upper-convective derivative. Governing equation is formulated where the space fractional derivative is characterized by the weight coefficient of forward versus backward transition probability and solved by L1-approximation and shifted Grünwald formula. Results show that the fractional parameters, time and location parameters, relaxation parameter, weight coefficient and convection velocity have remarkable impacts on heat transfer characteristics. Temperature distribution profiles are monotonically decreasing in a concave form versus time fractional parameter under relaxation parameter exists, while in a convex form with space fractional parameter evolution under three special conditions, i.e., the right region, the larger weight coefficient (γ>=0.5) and smaller convection parameter u.

Keywords: Heat conduction, Cattaneo-Christov flux, fractional derivative.

1. Introduction

A considerable attention has been devoted to heat conduction [1-3] due to its extensive application in widespread fields. The classical 1-D constitutive model to describe heat conduction is deduced by the Fourier's law [4] which provides a way to study heat conduction and becomes the

*Corresponding author. Tel. (8610)62332891
Email addresses: liancunzheng@ustb.edu.cn

basis to study the heat transfer process in the past few years. However, a paradox for the Fourier's model [5-7] is that it is felt instantly throughout the whole of the medium even for small times. This behavior contradicts the principle of causality [8-9] which issued an infinite propagation velocity. In order to overcome this problem, a modified constitutive model is proposed by Cattaneo [10] which takes the relaxation parameter into account.

The Cattaneo constitutive relation only involves partial time derivative, higher spatial gradients may be required [11] for a complete process. Revising the time derivative as the Oldroyds' upper-convected derivative, Christov [12] proposed the frame-indifferent generalization of Cattaneo model:

$$\mathbf{q}+\xi\left[\frac{\partial \mathbf{q}}{\partial t}+\mathbf{V}\cdot\nabla\mathbf{q}-\mathbf{q}\cdot\nabla\mathbf{V}+\left(\nabla\cdot\mathbf{V}\right)\mathbf{q}\right]=-k\,\mathrm{grad}\,T\,, \tag{1}$$

where $\mathbf{q}$, $\mathbf{V}$, k, ξ and T refer to heat flux vector, velocity vector, thermal conductivity, relaxation parameter and temperature distribution function, respectively. The propagation velocity [13] is defined as $v=\left(D/\xi\right)^{1/2}$, and it reduces to the classical Fourier's law with an infinite propagation velocity for $\xi\to 0$. The new flux model satisfies the objectivity principle and attracts a large number of scholars' attention. Straughan [14] considered the thermal convection in a horizontal layer of incompressible Newtonian fluid with gravity acting downward. Using Cattaneo–Christov heat flux model, Han et al. [15] studied coupled flow and heat transfer of an upper-convected Maxwell fluid above a stretching plate, analyzing the dynamic property with different parameters effect and presenting a comparison of Fourier's Law and the Cattaneo–Christov heat flux model. Basing upon Cattaneo–Christov theory, Hayat et al. [16] considered temperature dependent thermal conductivity in stagnation point flow toward a nonlinear stretched surface with variable thickness, results showed that temperature profile decreases for higher thermal relaxation parameter. Sui et al. [17] introduced the Cattaneo–Christov model to study and analyze the boundary layer heat and mass transfer in upper-convected Maxwell nanofluid past a stretching sheet with slip velocity. More literatures related to Cattaneo–Christov model can be seen in Refs. [18-21].

Fractional-order partial differential equation is a generalization and development of integer order one. The fractional derivative indicates that the position we consider is not only depended on its nearby positions but also on the whole positions, while the integer order operator is only a local one. For the time fractional derivative, Du et al. [22] indicated that its physical meaning is an index of memory. The space one reflects a non-local character and it can describe transfer process in a highly inhomogeneous medium more adequately by comparing with experiment data [23]. The study for the application of fractional derivative operator has attracted considerable attentions. Zaslavsky [24] reviewed the new concept of fractional kinetics for systems with Hamiltonian chaos, proving that fractional kinetics is valuable in different important physical phenomena. Henry et al. [25] introduced the temporal fractional cable equations to model electrotonic properties of spiny neuronal dendrites, predicting that postsynaptic potentials propagating can arrive at the soma faster along dendrites with larger spine densities and be sustained at higher levels over longer times. Chen et al. [26] proposed variable-order fractional derivative model which can agree significantly better with experimental data. For more references about the application of fractional operators, see in Refs. [27-29].

Motivated by above mentioned discussions, we firstly extend the study of heat conduction with time and space fractional Cattaneo-Christov equation. By considering the velocity as a constant and the generalized derivative of time [13] and space fractional order [30], Eq. (1) can be rewritten into the following one dimensional form:

$$\mathrm{q}+\xi\left(\tau^{\alpha-1}\frac{\partial^{\alpha}\mathrm{q}}{\partial t^{\alpha}}+u\frac{\partial \mathrm{q}}{\partial x}\right)=-k\left(\gamma\frac{\partial^{\beta}T(x,t)}{\partial x^{\beta}}-(1-\gamma)\frac{\partial^{\beta}T(x,t)}{\partial(-x)^{\beta}}\right), \tag{2}$$

where τ is introduced to keep the dimension of constitutive equation balance and its dimension is " s ", u is the convection velocity along the x direction, γ ($0\le\gamma\le1$) is the weight coefficient of forward versus backward transition probability, the symbol $\frac{\partial^{\alpha}}{\partial t^{\alpha}}$ is the Caputo's time fractional derivative [31] of order α ($0<\alpha\le1$), defined as:

$$\frac{\partial^{\alpha}T(x,t)}{\partial t^{\alpha}}=\frac{1}{\Gamma(1-\alpha)}\int_{0}^{t}\frac{1}{(t-\tau)^{\alpha}}\frac{\partial T(x,\tau)}{\partial\tau}d\tau, \tag{3}$$

where the symbol $\Gamma(\cdot)$ represents the Euler gamma function.

The symbols $\frac{\partial^{\beta}}{\partial x^{\beta}}$ and $\frac{\partial^{\beta}}{\partial(-x)^{\beta}}$ are the left and right Riemann-Liouville fractional derivatives of order β ($0<\beta\le 1$), the corresponding definitions [32] on a finite domain $[a,b]$ are given by:

$$\frac{\partial^{\beta}T(x,t)}{\partial x^{\beta}}=\frac{1}{\Gamma(1-\beta)}\frac{\partial}{\partial x}\int_{a}^{x}(x-\xi)^{-\beta}T(\xi,t)\,d\xi\,, \tag{4}$$

and

$$\frac{\partial^{\beta}T(x,t)}{\partial(-x)^{\beta}}=\frac{-1}{\Gamma(1-\beta)}\frac{\partial}{\partial x}\int_{x}^{b}(\xi-x)^{-\beta}T(\xi,t)\,d\xi\,, \tag{5}$$

respectively.

2. Mathematical formulation

First, we give the mass conservation equation:

$$c\rho\frac{\partial T}{\partial t}+c\rho u\frac{\partial T}{\partial x}+\mathrm{div}\,q=\,, \tag{6}$$

where c and ρ are the specific heat capacity and mass density, respectively.

By the combination of (2) and (6), one arrives at the time and space fractional Cattaneo-Christov heat conduction equation:

$$\begin{aligned}&\xi\tau^{\alpha-1}\frac{\partial^{1+\alpha}T}{\partial t^{1+\alpha}}+\xi u\tau^{\alpha-1}\frac{\partial^{\alpha+1}T}{\partial x\partial t^{\alpha}}+\xi u\frac{\partial^{2}T}{\partial x\partial t}+\frac{\partial T}{\partial t}+u\frac{\partial T}{\partial x}+\xi u^{2}\frac{\partial^{2}T}{\partial x^{2}}\\&-D\frac{\partial}{\partial x}\left[\gamma\frac{\partial^{\beta}T}{\partial x^{\beta}}-(1-\gamma)\frac{\partial^{\beta}T}{\partial(-x)^{\beta}}\right]=0\end{aligned}\,, \tag{7}$$

with the initial and boundary conditions:

$$T(x,0)=\frac{1}{L^{4}}x^{2}(L-x)^{2},\quad \frac{\partial T(x,0)}{\partial t}=0\,, \tag{8}$$

and

$$T(0,t)=T(L,t)=\,, \tag{9}$$

respectively. Here $D=k/(c\rho)$ is the thermal diffusivity coefficient. For the sake of simplifying our study, the non-dimensional quantities are introduced:

$$t\to\tau t^{*},x\to Lx^{*},\xi\to\tau\xi^{*},u\to\frac{L}{\tau}u^{*},r\to\frac{L^{\beta+1}}{\tau D}r^{*},1-r\to\frac{L^{\beta+1}}{\tau D}\left(1-r^{*}\right). \tag{10}$$

Submitting the non-dimensional quantities into (7)-(9), we can obtain the dimensionless governing equation with initial and boundary conditions (the superscript * is omitted for simplicity):

$$\begin{aligned}&\xi\frac{\partial^{1+\alpha}T}{\partial t^{1+\alpha}}+\xi u\frac{\partial^{\alpha+1}T}{\partial x\partial t^{\alpha}}+\xi u\frac{\partial^{2}T}{\partial x\partial t}+\frac{\partial T}{\partial t}+u\frac{\partial T}{\partial x}+\xi u^{2}\frac{\partial^{2}T}{\partial x^{2}}\\&-\left[\gamma\frac{\partial^{\beta+1}T}{\partial x^{\beta+1}}+\left(1-\gamma\right)\frac{\partial^{\beta+1}T}{\partial\left(-x\right)^{\beta+1}}\right]=0\end{aligned},\tag{11}$$

$$T\left(x,0\right)=x^{2}\left(1-x\right)^{2},\quad\frac{\partial T\left(x,0\right)}{\partial t}=0,\tag{12}$$

$$T\left(0,t\right)=T\left(1,t\right)=\ .\tag{13}$$

By setting $\beta=1$ and $u=0$, Eq. (11) reduces to the time fractional Cattaneo model [8] while Eq. (11) reduces to the classical heat conduction model [4] when $\beta=1$, $\xi=0$ and $u=0$.

3. Numerical discretization method

Firstly, we define $x_i=ih$ ($i=0,1,2,...,m$, $mh=1$) and $t_j=j\tau$ ($j=0,1,2,...,n$) where h is the grid size in space and τ is grid size in time. Prior to obtaining the numerical solution of Eq. (11), some useful definitions of difference scheme for the time and space fractional derivative are presented.

The Caputo fractional derivative of order $0<\alpha\le 1$ with respect to time at $t=t_j$ is approximated by L1-approximation [33], the discrete scheme is given as follows:

$$\begin{aligned}&\frac{\partial^{\alpha}T\left(x,t_j\right)}{\partial t^{\alpha}}\\&\approx\frac{1}{\tau^{\alpha}\Gamma\left(2-\alpha\right)}\left[T\left(x_i,t_j\right)+\sum_{k=1}^{j-1}\left(c_{j-k}-c_{j-k-1}\right)T\left(x_i,t_k\right)-c_{j-1}T\left(x_i,t_0\right)\right]\end{aligned},\tag{14}$$

where $c_0=1$, $c_k=\left(k+1\right)^{1-\alpha}-k^{1-\alpha}$, $k=1,2,...$.

On the basis of L1-approximation, the Caputo fractional derivative of order $1<1+\alpha\le 2$ can be deduced by:

$$
\begin{aligned}
&\frac{\partial^{1+\alpha} T\left(x, t_j\right)}{\partial t^{1+\alpha}} \\
&\approx \frac{1}{\tau^{1+\alpha}\Gamma(2-\alpha)}\left[c_0\left(T\left(x_i, t_j\right)-T\left(x_i, t_{j-1}\right)\right)-\sum_{l=1}^{j-1}(c_{j-l-1}-c_{j-l})\left(T\left(x_i, t_l\right)-T\left(x_i, t_{l-1}\right)\right)\right].
\end{aligned}
\tag{15}
$$

The shifted Grünwald formulae [34] to approximate the space fractional derivative of order $1<\beta+1\leq 2$ are given by:

$$
\frac{\partial^{\beta+1} T\left(x_i, t_j\right)}{\partial x^{\beta+1}} \approx \frac{1}{h^{\beta+1}} \sum_{l=0}^{i+1} \omega_l^{\beta+1} T\left(x_{i-l+1}, t_j\right), \tag{16}
$$

$$
\frac{\partial^{\beta+1} T\left(x_i, t_j\right)}{\partial (-x)^{\beta+1}} \approx \frac{1}{h^{\beta+1}} \sum_{l=0}^{m-i+1} \omega_l^{\beta+1} T\left(x_{i+l-1}, t_j\right), \tag{17}
$$

where the symbol $\omega_l^{\beta+1}$ refer to the Grünwald weight coefficient and $\omega_0^{\beta+1}=1$, $\omega_l^{\beta+1}=\left(1-\frac{\beta+2}{l}\right)\omega_{l-1}^{\beta+1}$.

On the basis of the above discrete schemes, meanwhile, using the backward difference scheme for the first order space and time derivatives and the central difference scheme for the second order space derivative at the mesh point $\left(x_i, t_j\right)$, we can obtain the final discrete scheme of (11) in the form:

$$
\begin{aligned}
&-\frac{1-\gamma}{h^{\beta+1}} \sum_{l=i+2}^{m} \omega_{l-i+1}^{\beta+1} T_l^j+\left(\frac{\xi u^2}{h^2}-\frac{\gamma}{h^{\beta+1}} \omega_0^{\beta+1}-\frac{1-\gamma}{h^{\beta+1}} \omega_2^{\beta+1}\right) T_{i+1}^j \\
&+\left[r_1+r_2-2 \frac{\xi u^2}{h^2}+\frac{1}{\tau}+\frac{u}{h}+\frac{\xi u}{h \tau}-\frac{1}{h^{\beta+1}} \omega_1^{\beta+1}\right] T_i^j \\
&+\left[\frac{\xi u^2}{h^2}-r_2-\frac{\xi u}{h \tau}-\frac{u}{h}-\frac{\gamma}{h^{\beta+1}} \omega_2^{\beta+1}-\frac{1-\gamma}{h^{\beta+1}} \omega_0^{\beta+1}\right] T_{i-1}^j-\frac{\gamma}{h^{\beta+1}} \sum_{l=0}^{i-2} \omega_{i-l+1}^{\beta+1} T_l^j, \\
&=\frac{\xi u}{h \tau}\left(T_i^{j-1}-T_{i-1}^{j-1}\right)+\frac{1}{\tau} T_i^{j-1}+r_1\left[T_i^{j-1}-\sum_{l=1}^{j-1}(c_{j-l}-c_{j-l-1})\left(T_i^l-T_i^{l-1}\right)\right] \\
&-r_2\left[\sum_{k=1}^{j-1}\left(c_{j-k}-c_{j-k-1}\right)\left(T_i^k-T_{i-1}^k\right)-c_{j-1}\left(T_i^0-T_{i-1}^0\right)\right]
\end{aligned}
\tag{18}
$$

where $r_1=\frac{\xi}{\tau^{1+\alpha}\Gamma(2-\alpha)}$ and $r_2=\frac{\xi u}{\tau^{\alpha}\Gamma\left(2-\alpha\right)h}$.

By defining new matrixes G and A:

$$
G_{il}=\begin{cases}-\dfrac{1-\gamma}{h^{\beta+1}}\omega_{l-i+1}^{\beta+1} & l\ge i+2,\\ \dfrac{\xi u^2}{h^2}-\dfrac{\gamma}{h^{\beta+1}}\omega_0^{\beta+1}-\dfrac{1-\gamma}{h^{\beta+1}}\omega_2^{\beta+1} & l=i+1,\\ r_1+r_2-2\dfrac{\xi u^2}{h^2}+\dfrac{1}{\tau}+\dfrac{u}{h}+\dfrac{\xi u}{h\tau}-\dfrac{1}{h^{\beta+1}}\omega_1^{\beta+1} & l=i,\\ \dfrac{\xi u^2}{h^2}-r_2-\dfrac{\xi u}{h\tau}-\dfrac{u}{h}-\dfrac{\gamma}{h^{\beta+1}}\omega_2^{\beta+1}-\dfrac{1-\gamma}{h^{\beta+1}}\omega_0^{\beta+1} & l=i-1,\\ -\dfrac{\gamma}{h^{\beta+1}}\omega_{i-l+1}^{\beta+1} & l\le i-2,\end{cases} \tag{19}
$$

and

$$
A=\begin{pmatrix}1 & & & & & \\ -1 & 1 & & & & \\ & -1 & 1 & & & \\ & & \ddots & \ddots & & \\ & & & -1 & 1 & \\ & & & & -1 & 1\end{pmatrix}_{M\times M}, \tag{20}
$$

Eq. (18) can be simplified as:

$$
\begin{aligned}GT^{j}&=\frac{\xi u}{h\tau}AT^{j-1}+\frac{1}{\tau}T^{j-1}+r_1\left[T^{j-1}-\sum_{l=1}^{j-1}(c_{j-l}-c_{j-l-1})\left(T^{l}-T^{l-1}\right)\right]\\&-r_2\left[\sum_{k=1}^{j-1}\left(c_{j-k}-c_{j-k-1}\right)AT^{k}-c_{j-1}AT^{0}\right].\end{aligned} \tag{21}
$$

The initial condition and boundary condition are discretized as:

$$
T_i^0=x_i^2\left(1-x_i\right)^2,\quad T_i^0=T_i^1,\quad i=1,2,\dots,m-1 \tag{22}
$$

and

$$
T_0^j=0,\quad T_m^j=0,\quad j=0,1,2,\dots,n, \tag{23}
$$

respectively.

4. Comparison between analytical and numerical solutions in the special case

In order to verify the correctness of numerical discretization method, we construct the following governing equation by introducing a source item $f\left(x,t\right)$:

$$
\xi\frac{\partial^{1+\alpha}T}{\partial t^{1+\alpha}}+\xi u\frac{\partial^{\alpha+1}T}{\partial x\partial t^{\alpha}}+\xi u\frac{\partial^2 T}{\partial x\partial t}+\frac{\partial T}{\partial t}+u\frac{\partial T}{\partial x}+\xi u^2\frac{\partial^2 T}{\partial x^2}-\left[\gamma\frac{\partial^{\beta+1}T}{\partial x^{\beta+1}}+\left(1-\gamma\right)\frac{\partial^{\beta+1}T}{\partial(-x)^{\beta+1}}\right]=f\left(x,t\right), \tag{24}
$$

subject to initial condition (12) and boundary conditions (13), where

$$
\begin{aligned}
& f(x,t) \\
&= 2\left[\frac{\xi}{\Gamma(2-\alpha)}t^{-\alpha}+1\right]x^2(1-x)^2 t + 2\xi u^2\left(1-6x+6x^2\right)\left(t^2+1\right) \\
&+ 2ux(1-x)(1-2x)\left[\frac{2\xi t^{2-\alpha}}{\Gamma(3-\alpha)}+2\xi t+t^2+1\right] \\
&- \left\{\begin{aligned} &\gamma\left(t^2+1\right)\left[\frac{\Gamma(3)}{\Gamma(2-\beta)}x^{1-\beta}-2\frac{\Gamma(4)}{\Gamma(3-\beta)}x^{2-\beta}+\frac{\Gamma(5)}{\Gamma(4-\beta)}x^{3-\beta}\right] \\ &+(1-\gamma)\left(t^2+1\right)\left[\frac{\Gamma(3)}{\Gamma(2-\beta)}(-x)^{1-\beta}+2\frac{\Gamma(4)}{\Gamma(3-\beta)}(-x)^{2-\beta}+\frac{\Gamma(5)}{\Gamma(4-\beta)}(-x)^{3-\beta}\right]\end{aligned}\right\}
\end{aligned}, \qquad (25)
$$

and the exact solution is $T(x,t)=\left(t^2+1\right)x^2(1-x)^2$.

The comparison results of exact solution and numerical solution are shown in Fig. 1. The comparison curves fit very well which can indicate the correctness of numerical results.

5. Results and discussion

Time fractional derivative provides an adequate description of memory properties of heat conduction while the space one reflects nonlocality in a complex medium. In this section, we mainly discuss the influences of different parameters on temperature distribution versus fractional parameters α and β. For the sake of simplicity, we discuss effects of α and β in a closed domain $[0.1,1]$. Two monotonically decreasing forms of temperature distribution are presented: one is for time fractional parameter evolution, the distributions are presented as a concave form with relaxation parameter, meaning that the distribution decreases less dynamically at smaller α while more dynamically at larger one; the other is for space fractional parameters evolution, under the condition that $x \geq 0.5$, $\gamma \geq 0.5$ and u is smaller, the distributions are presented as a convex form, indicating that the distribution decreases from faster to slower with the increase of β.

Figs. 2-3 present the temperature distribution versus α and β with different values of x. Fig. 2 shows that the larger the x is, for smaller α, the smaller the magnitude of the distribution will be. With the increase of α, the distributions are monotonically decreasing in a concave form and the distribution falls faster for a smaller x. For larger α, it is worth noting that the smallest distribution corresponds to $x = 0.5$, which is the middle and highest position in the region we consider. The influences of x on temperature distribution versus β are presented in Fig. 3. It can be seen from the figure that the larger the x is, the larger the magnitude of the distribution will be at smaller β and the faster the distribution will fall. It is noteworthy that there exists a upward tendency for x=0.4, that we can suppose there exists a upward tendency for the left region $[0, 0.5)$. For x in the right region $\left[0.5, 1\right]$, the distributions are monotonically decreasing in a convex form with β increases. When $\beta \to 1$, the distributions change to flatten.

The temperature distributions versus α and β with different values of t are shown in Figs. 4-5. As Fig. 4 shows, the distributions versus α are monotonically decreasing in a concave form. The smaller the t is, the larger the magnitude of the distribution at smaller α will be and the faster the distributions will fall. Then, at larger α, the magnitude becomes smaller. The distributions versus β in a convex form are shown in Fig. 5. For a smaller t, the magnitude of the distribution is larger at smaller β and the distribution decreases more dramatically. For $\beta \to 1$, the larger the t is, the larger the magnitude of the distribution will be. It can be seen from the figure that the distributions are monotonically decreasing for $t = 0.4$ and $t = 0.5$, while there exists a upward tendency for $t = 0.6$.

Figs. 6-7 present the time and space fractional parameters evolution of temperature distribution under the influences of different values of γ. It can be seen from Eq. (11) that the diffusion term along the x direction is combined by the left and right terms with forward and backward weight coefficients. For $\gamma = 1/2$, the left and right weight coefficients are equal. For $\gamma > 1/2$, the left weight coefficient is larger than the right one while the right coefficient is larger for $\gamma < 1/2$. The larger left (right) coefficient means a larger weight for the non-local left (right) heat transfer. Fig. 6 shows that the distributions are monotonically decreasing versus α in a concave form. The smaller the γ is, the larger the magnitude of the distribution will be, but the changes are not obvious. For $\gamma = 1/2$ and $\gamma = 3/4$, as Fig. 7 shows, the distributions versus

β are monotonically decreasing in a convex form. It is noteworthy that there exists a upward tendency for $\gamma = 1/4$ at smaller β. For a larger γ, the magnitude of the distribution is larger at smaller β and the distribution decreases faster with the increase of β. For larger β, the distribution becomes smaller at a larger γ and the distributions begin to flatten when $\beta \to 1$.

The time and space fractional parameters evolution of temperature distribution with different values of u are respectively presented in Fig. 8 and Fig. 9. For $u = 0$, (11) reduces to the time and space fractional Cattaneo heat conduction equation. Fig. 8 shows that the distributions versus α are monotonically decreasing in a concave form. For a larger u, the magnitude of the distribution is larger at smaller α and the larger the u is, the faster the distribution will decrease. And the magnitude becomes smaller for larger α (near to $\alpha = 1$). Fig. 9 shows that the distributions versus β with different values of u are monotonically decreasing in a convex form for $u = 0$ and $u = 0.3$ while there exists a upward tendency for $u = 0.6$. We can conclude that the larger u can change the concavity and convexity of the temperature distribution. For a smaller u, the magnitude of the distribution is larger at smaller β and falls faster with β increases. When $\beta \to 1$, the distributions change to flatten.

6. Conclusions

Time and space fractional Cattaneo-Christov constitutive model is proposed to describe heat conduction. Solutions of formulated governing equation are obtained numerically and the comparison of numerical solution and exact solution is presented by introducing a source term. The influences of related parameters on time and space fractional parameters evolution of temperature distribution are analyzed in detail. Results show that the temperature profiles are monotonically decreasing in a concave form with time fractional parameter evolution with relaxation parameter, while in a convex form versus space fractional parameter when $x \geq 0.5$, $\gamma \geq 0.5$ and u is smaller. Further research is needed to verify the effectiveness of fractional Cattaneo-Christov heat conduction model with experimental data.

Acknowledgement. The work is supported by the National Natural Science Foundations of China (No. 51276014, 51476191).

References

[1] Özisik MN. Heat Conduction, third ed., John Wiley & Sons, New York, 1993.

[2] Garrido PL, Hurtado PI, Nadrowski B. Simple One-Dimensional Model of Heat Conduction which Obeys Fourier's Law. Phys Rev Lett 2001; 86: 5486-9.

[3] Kabir MM. Analytic solutions for generalized forms of the nonlinear heat conduction equation. Nonlinear Anal RWA 2011; 12: 2681–91.

[4] Guo SL, Wang BL. Thermal shock fracture of a cylinder with a penny-shaped crack based on hyperbolic heat conduction. Int J Heat Mass Tran 2015; 91: 235–45.

[5] Christov CI, Jordan PM. Heat Conduction Paradox Involving Second-Sound Propagation in Moving Media. Phys Rev Lett 2005; 94: 154301.

[6] Qi HT, Guo XW. Transient fractional heat conduction with generalized Cattaneo model. Int J Heat Mass Tran 2014; 76: 535-39.

[7] Xu HY, Qi HT, Jiang XY. Fractional Cattaneo heat equation in a semi-infinite medium. Chin Phys B 2013; 22: 014401-1-6.

[8] Zhao X, Sun ZZ. Compact Crank–Nicolson Schemes for a Class of Fractional Cattaneo Equation in Inhomogeneous Medium. J Sci Comput 2015; 62: 747-71.

[9] Qi HT, Jiang XY. Solutions of the space-time fractional Cattaneo diffusion equation. Physica A 2011; 390: 1876-83.

[10] Cattaneo C. Sulla conduzione del calore, Atti Semin. Mat. Fis. Univ. Modena Reggio Emilia, 1948; 3: 83-101.

[11] Liu L, Zheng LC, Zhang XX. Fractional anomalous diffusion with Cattaneo–Christov flux effects in a comb-like structure. Appl Math Model 2016; 40: 6663–75.

[12] Christov CI. On frame indifferent formulation of the Maxwell–Cattaneo model of finite-speed heat conduction. Mech Res Commun 2009; 36: 481-6.

[13] Compte A, Metzler R. The generalized Cattaneo equation for the description of anomalous transport processes. J Phys A Math. Gen 1997; 30: 7277-89.

[14] Straughan B. Thermal convection with the Cattaneo–Christov model. Int J Heat Mass Transfer

2010; 53: 95-8.

[15] Han SH, Zheng LC, Li CR, Zhang XX. Coupled flow and heat transfer in viscoelastic fluid with Cattaneo–Christov heat flux model. Appl Math Lett 2014; 38: 87-93.

[16] Hayat T, Ijaz Khan M, Farooq M, Alsaedi A, Waqas M, Yasmeen T. Impact of Cattaneo–Christov heat flux model in flow of variable thermal conductivity fluid over a variable thicked surface. Int J Heat Mass Tran 2016; 99: 702–10.

[17] Sui JZ, Zheng LC, Zhang XX. Boundary layer heat and mass transfer with Cattaneo-Christov double-diffusion in upper-convected Maxwell nanofluid past a stretching sheet with slip velocity. Int J Therm Sci 2016; 104: 461-8.

[18] Tibullo V, Zampoli V. A uniqueness result for the Cattaneo–Christov heat conduction model applied to incompressible fluids. Mech Res Commun 2011; 38: 77-9.

[19] Haddad SAM. Thermal instability in Brinkman porous media with Cattaneo–Christov heat flux. Int J Heat Mass Tran 2014; 68: 659-68.

[20] Liu L, Zheng LC, Liu FW, Zhang XX. Anomalous convection diffusion and wave coupling transport of cells on comb frame with fractional Cattaneo–Christov flux. Commun Nonlinear Sci 2016; 38: 45–58.

[21] Li J, Zheng LC, Liu L. MHD viscoelastic flow and heat transfer over a vertical stretching sheet with Cattaneo-Christov heat flux effects. J Mol Liq 2016; 221: 19–25.

[22] Du ML, Wang ZH, Hu HY. Measuring memory with the order of fractional derivative. Sci Rep 2013; 3: 1-3.

[23] Benson DA, Wheatcraft SW, Meerschaert MM. Application of a fractional advection-dispersion equation. Water Resour Res 2000; 36: 1403–1412.

[24] Zaslavsky GM. Chaos, fractional kinetics, and anomalous transport. Phys Rep 2002; 371: 461–580.

[25] Henry BI, Langlands TAM, Wearne SL. Fractional Cable Models for Spiny Neuronal Dendrites. Phys Rev Lett 2008; 100: 1-4.

[26] Chen W, Zhang JJ, Zhang JY. A variable-order time-fractional derivative model for chloride ions sub-diffusion in concrete structures. Fract Calc Appl Anal 2013; 16: 76-92.

[27] Jiang XY, Qi HT. Thermal wave model of bioheat transfer with modified Riemann–Liouville fractional derivative. J Phys A Math Theor 2012; 45: 1-11.

[28] Fan WP, Jiang XY, Qi HT. Parameter estimation for the generalized fractional element network Zener model based on the Bayesian method. Physica A 2015; 427: 40–49.

[29] Yu B, Jiang XY, Xu HY. A novel compact numerical method for solving the two-dimensional non-linear fractional reaction-subdiffusion equation. Numer Algor 2015; 68: 923–950.

[30] Hejazi H, Moroney T, Liu FW. Stability and convergence of a finite volume method for the space fractional advection–dispersion equation. J Comput Appl Math 2014; 255: 684-97.

[31] Podlubny I. Fractional Differential Equations, Academic Press, New York, 1999.

[32] Feng LB, Zhuang P, Liu F, Turner I, Stability and convergence of a new finite volume method for a two-sided space-fractional diffusion equation. Appl Math Comput 2015; 257: 52-65.

[33] Langlands TAM, Henry BI. The accuracy and stability of an implicit solution method for the fractional diffusion equation. J Comput Phys 2005; 205: 719-36.

[34] Liu F, Zhuang P, Burrage K. Numerical methods and analysis for a class of fractional advection–dispersion models. Comput Math Appl 2012; 64: 2990-3007.

Figures list:

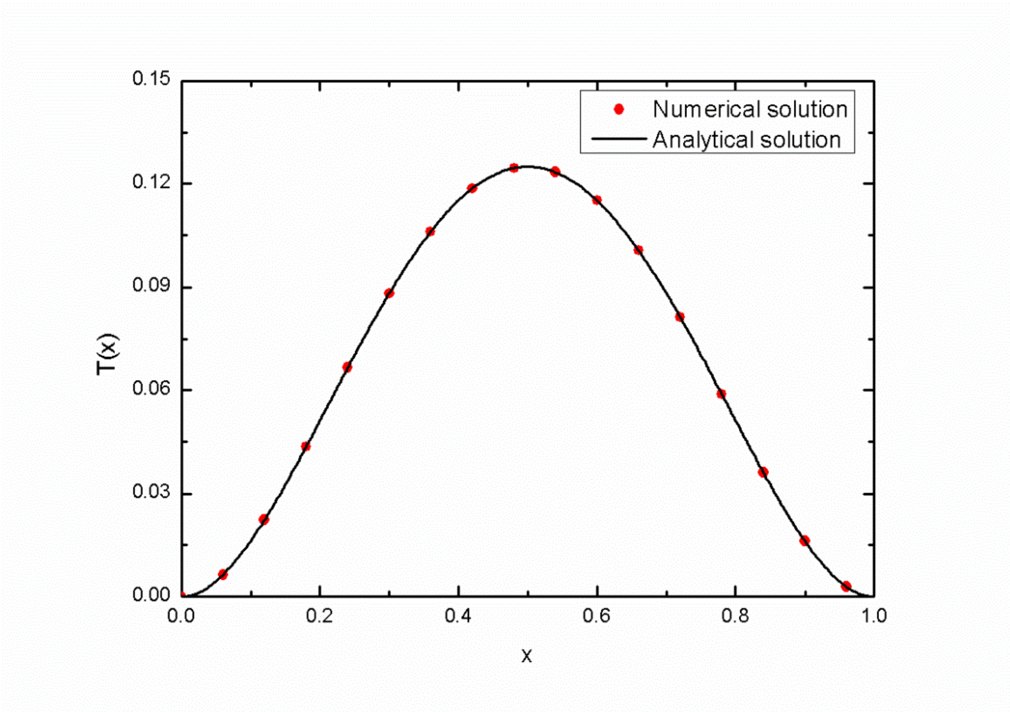

Fig. 1. The comparison between exact solution and numerical solution when $t=1$, $\xi=0.1$, $u=0.1$, $\alpha=1$, $\beta=1$ and $\gamma=1/2$.

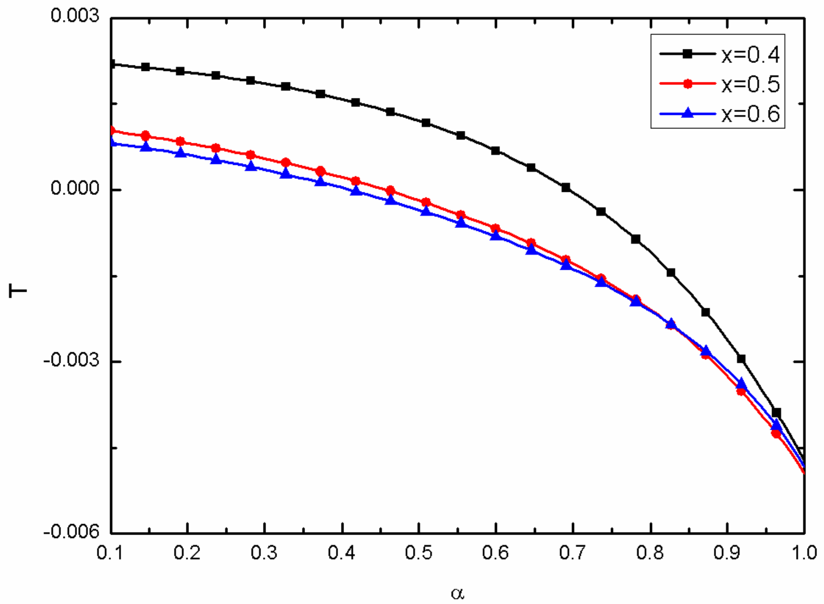

Fig. 2. The time fractional parameter evolution of temperature distribution with different values of x when $\xi = 0.1$, $\gamma = 1/2$, $\beta = 0.95$, $t = 0.5$ and $u = 0.5$.

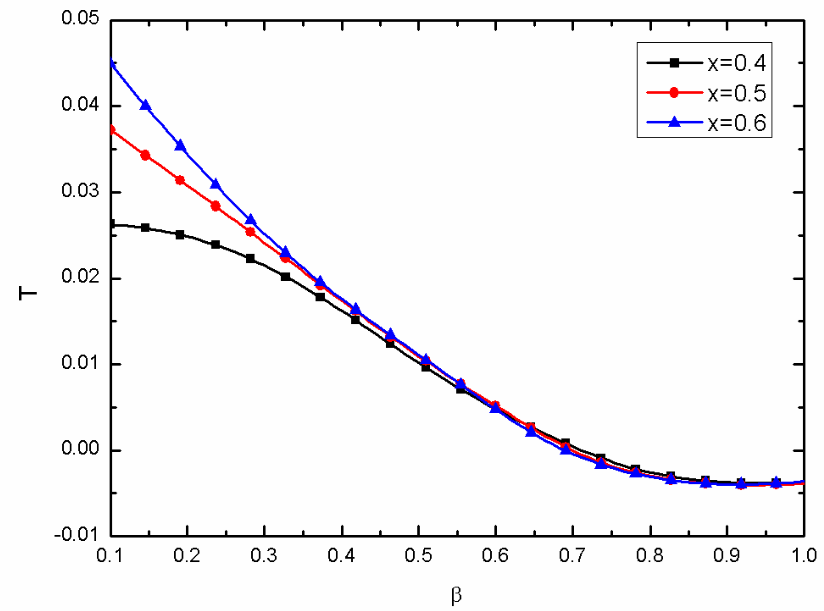

Fig. 3. The space fractional parameter evolution of temperature distribution with different values of x when $\xi = 0.1$, $\gamma = 1/2$, $\alpha = 0.95$, $t = 0.5$ and $u = 0.5$.

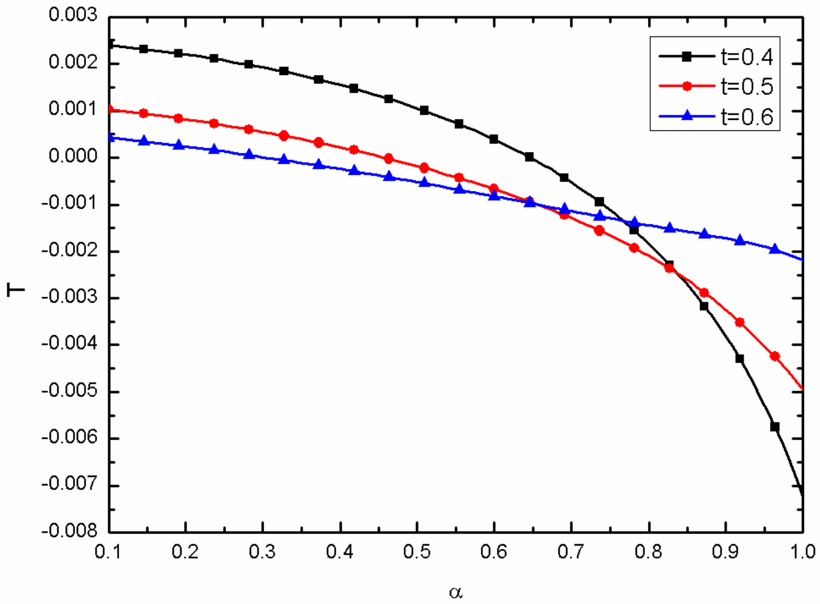

Fig. 4. The time fractional parameter evolution of temperature distribution with different values of t when $\xi = 0.1$, $\gamma = 1/2$, $x = 0.5$, $\beta = 0.95$ and $u = 0.5$.

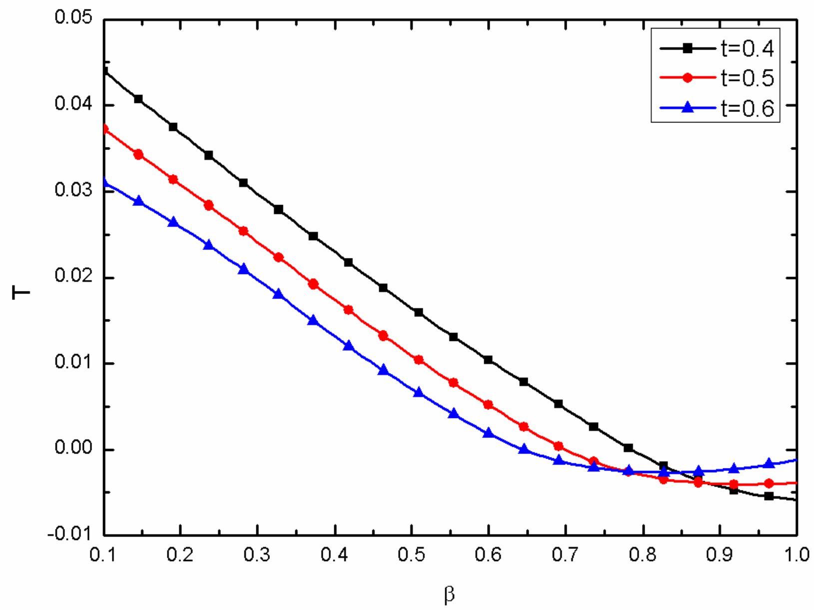

Fig. 5. The space fractional parameter evolution of temperature distribution with different values of t when $\xi = 0.1$, $\gamma = 1/2$, $x = 0.5$, $\alpha = 0.95$ and $u = 0.5$.

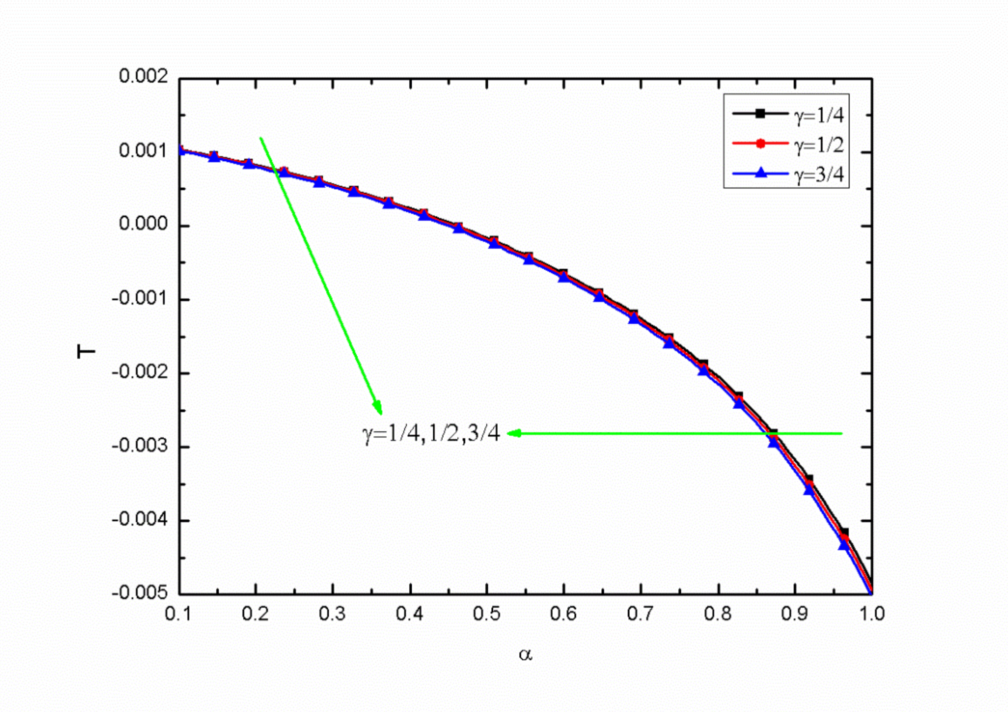

Fig. 6. The time fractional parameter evolution of temperature distribution with different values of γ when $\xi = 0.1$, $\beta = 0.95$, $x = 0.5$, $t = 0.5$ and $u = 0.5$.

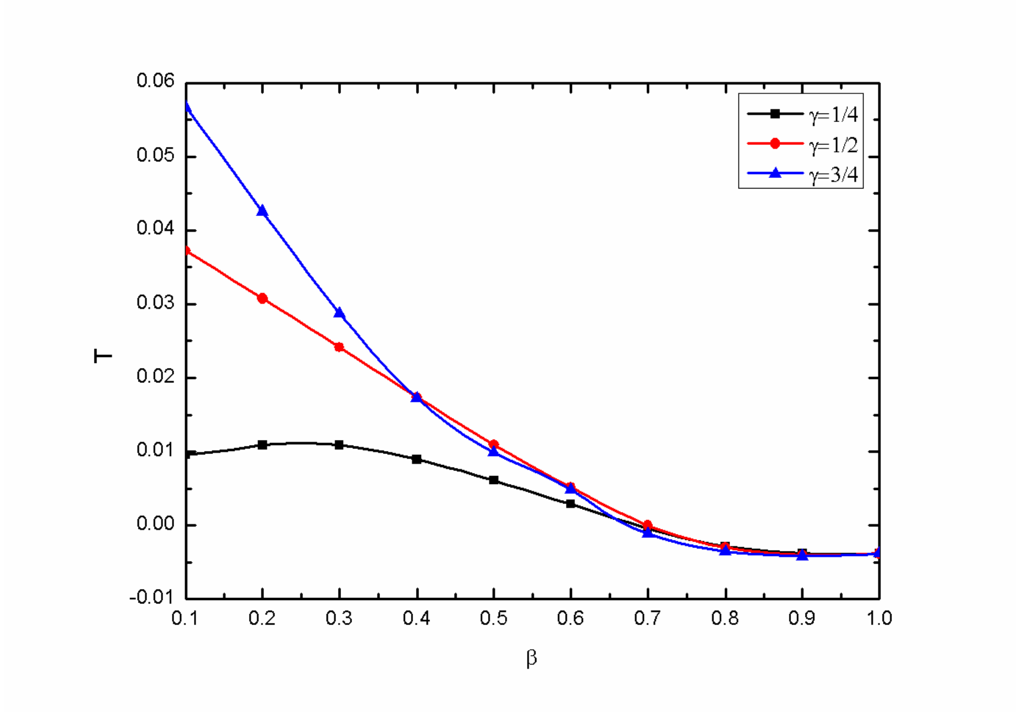

Fig. 7. The space fractional parameter evolution of temperature distribution with different values of γ when $\xi = 0.1$, $\alpha = 0.95$, $x = 0.5$, $t = 0.5$ and $u = 0.5$.

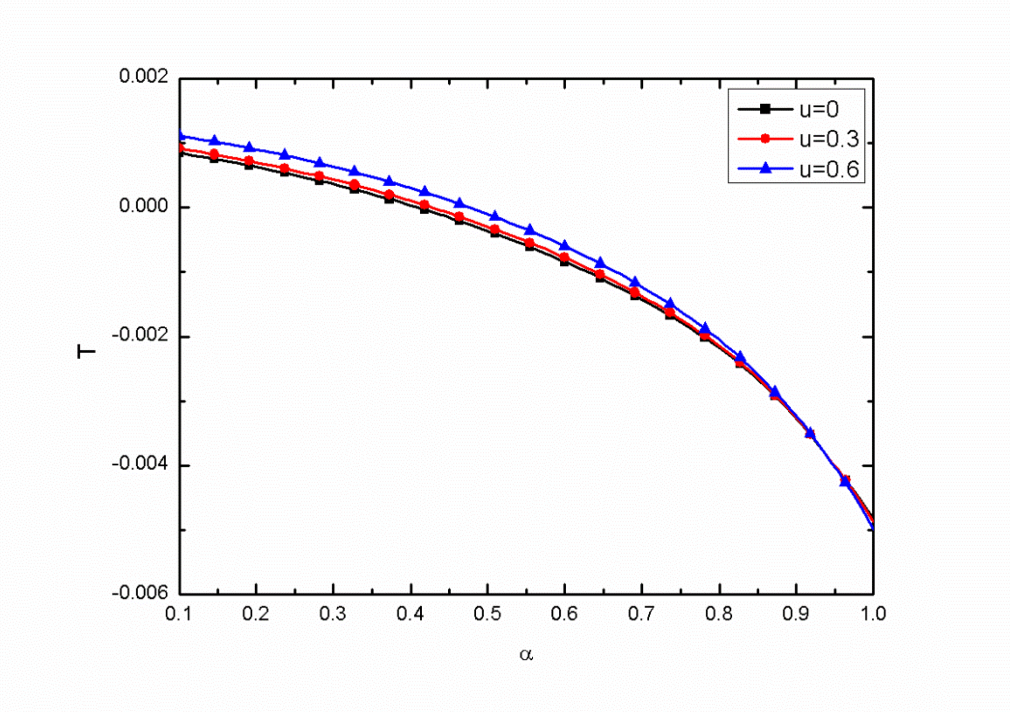

Fig. 8. The time fractional parameter evolution of temperature distribution with different values of u when $\xi = 0.1$, $\gamma = 1/2$, $x = 0.5$, $t = 0.5$ and $\beta = 0.95$.

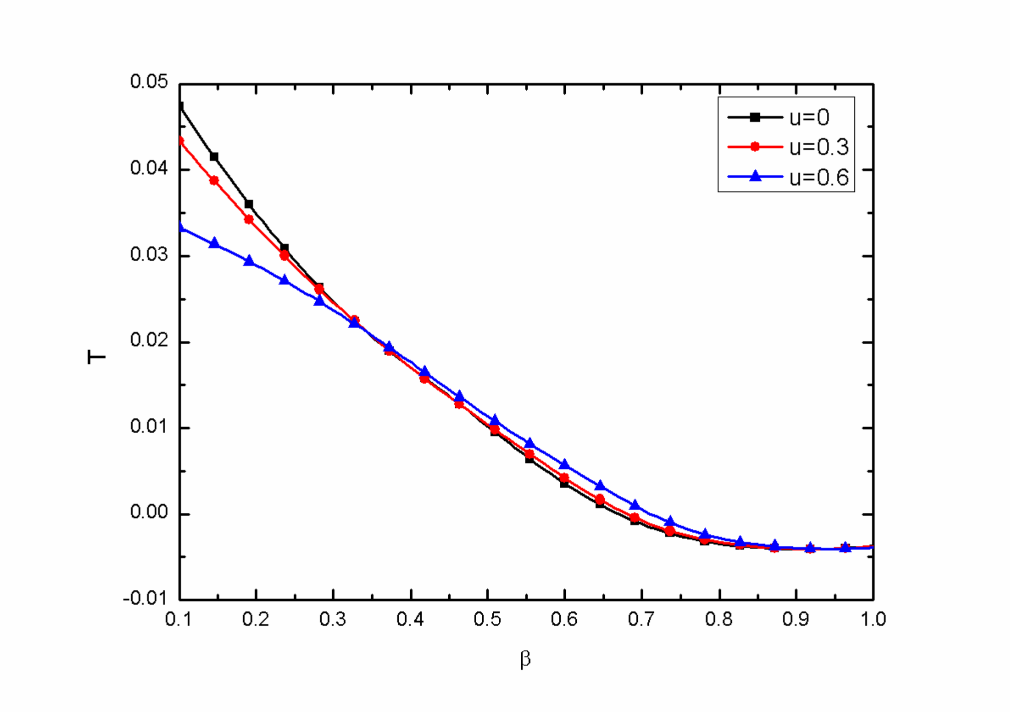

Fig. 9. The space fractional parameter evolution of temperature distribution with different values of u when $\xi = 0.1$, $\gamma = 1/2$, $x = 0.5$, $t = 0.5$ and $\alpha = 0.95$.